/N- 82A 19738
02

NASA TECHNICAL MEMORANDUM

NASA TM-76878

AERODYNAMICS ON A TRANSPORT AIRCRAFT TYPE WING-BODY MODEL

V. Schmitt

Translation of "Aerodynamique d'un ensemble voilure-fuselage du type 'avion de transport'", Office National d'Etudes et de recherches aerospatiales, Chatillon, France, Report ONERA T.P. 1981-122, (Paper presented at the 18th Colloquium on Applied Aerodynamics of AAAF, Poitiers, 18-20 November 1981), pp 1-23

NATIONAL AERONAUTICS AND SPACE ADMINISTRATION
WASHINGTON, D.C.   20546   MAY 1982

STANDARD TITLE PAGE

1. Report No. NASA TM-76878	2. Government Accession No.	3. Recipient's Catalog No.
4. Title and Subtitle AERODYNAMICS ON A TRANSPORT AIRCRAFT TYPE WING-BODY MODEL		5. Report Date MAY 1982
		6. Performing Organization Code
7. Author(s) V. Schmitt		8. Performing Organization Report No.
		10. Work Unit No.
9. Performing Organization Name and Address Leo Kanner Associates Redwood City, California 94063		11. Contract or Grant No. NASW-3541
		13. Type of Report and Period Covered Translation
12. Sponsoring Agency Name and Address National Aeronautics and Space Administration, Washington, D.C.20546		14. Sponsoring Agency Code

15. Supplementary Notes

Translation of "AERODYNAMIQUE D'UN ENSEMBLE VOILURE-FUSELAGE DU TYPE 'AVION DE TRANSPORT'", OFFICE NATIONAL D'ETUDES ET DE RECHERCHES AEROSPATIALES, Chatillon, France; Report ONERA T.P. 1981-122, (Paper presented at the 18th Colloquium on Applied Aerodynamics of AAAF, Poitiers, 18-20 November 1981), pp. 1-23.

16. Abstract This study carried out at ONERA is based on the DFLR-F4 wing-body combination. The 1/38 model is formed by a 9.5 aspect ratio transonic wing and an Airbus A 310 fuselage. This configuration has been selected as the main subject of a GAR-TEUR working group (cooperation between Germany, the Nether-lands, Great-Britain and France). The aim of this paper is to survey the work done by ONERA. After a description of the F4 wing geometrical characteristics, main experimental results obtained in the S2MA wind tunnel are discussed. Both wing-fuselage interferences and viscous effects, which are important on the wing due to a high rear loading, are investigated by performing 3D calculations. An attempt is made to find their limitations.

17. Key Words (Selected by Author(s))	18. Distribution Statement Unclassified-Unlimited
19. Security Classif. (of this report) Unclassified	20. Security Classif. (of this page) Unclassified	21. No. of Pages	22.

AERODYNAMICS ON A TRANSPORT AIRCRAFT TYPE WING-BODY MODEL

V. Schmitt

SUMMARY /1*

This study carried out at ONERA is based on the DFVLR-F4 wing-body combination. The 1/38 model is formed by a 9.5 aspect ratio transonic wing and an Airbus A 310 fuselage. This configuration has been selected as the main subject of a GARTEUR working group (cooperation between Germany, Netherlands, Great-Britain and France).

The aim of this paper is to survey the work done by ONERA. After a description of the F4 wing geometrical characteristics, main experimental results obtained in the S2MA wind tunnel are discussed. Both wing-fuselage interferences and viscous effects, which are important on the wing due to a high rear loading, are investigated by performing 3D calculations. An attempt is made to find their limitations.

1 - INTRODUCTION /2

The future development of the civilian transport aircraft in Europe, in the light of remaining competitive in the world market, will require more extensive studies to be conducted pertaining to the reduction of operating costs of such an aircraft. A special importance is, therefore, given to the development of methods of transonic calculation that are capable of handling an entire aircraft configuration. In this regard, considerable efforts have been made in Europe |1|, |2| and in the United States |3| , |4|,|5|. However, when geometric shapes become complex, the development of such methods and an accurate determination of their limitations also raise numerous and various types of problems.

One of the problems lies in the absence of a coherent and reliable set of experimental data, corresponding to a sufficiently realistic aircraft configuration, permitting an evaluation of calculation methods.

---

*Numbers in the margin indicate pagination in the foreign text.

In order to solve this problem, a working group formed under GARTEUR (Group for Aeronautical Research and Technology in Europe), which brings together representatives from research institutions and industries of France, Germany, Great Britain and the Netherlands, has decided to establish such a set of data. A model was selected for a wing-fuselage combination designed by DFVLR using the F4 advanced technology transonic wing and a 1/38 scale A 310 Airbus fuselage |6|.

This model is being tested in Europe's largest transonic wind tunnels and a comparison will be made of the various experimental results obtained. Furthermore, a comparison of these results with the results derived using some ten methods of transonic calculation will be another interesting aspect of this cooperation.

While awaiting the conclusions of the working group, that are expected to be available before the end of 1982, the purpose of this report is to provide a glimpse of ONERA's contribution to these works.

2 - DESIGN OF THE CONFIGURATION

The F4 wing was designed by DFVLR as a contribution to the ZKP (Ziviles Komponented Programm) research program started in Germany in 1975 with the financial support of the German Ministry for Research and Technology. This program, a few details of which are given in |7| , has been conducted in close collaboration between German aeronautic manufacturers and DFVLR for the purpose of providing a methodical contribution to transonic wing technology and minimizing the risks resulting from an application of this technology to civilian transport aircraft projects.

The conceptual design of the F4 wing is presented in detail in |8| and the essential points of it are presented in this chapter.

2.1 - Initial Conditions

The original intention was to design a transonic wing with a given conventional planar shape to be integrated with a fuselage provided with a passenger capacity of an Airbus A310. This planar shape is characterized by a tapered sweptback wing presenting a trailing edge break in such a manner to facilitate the integration of the landing gear into the wing (fig.1). The main parameters are:

aspect ratio	$\digamma$	= 9.5
taper ratio	V	= 0.3
sweep at trailing edge	φ_{9A}	=27.1°
break at trailing edge	y_c	=0.4 b/2
fuselage radius	r_f	=0.126 b/2

/3

The aerodynamic conditions to satisfy are as follows:

cruise Mach number (long distance)	M_o	= 0.785
coefficient of lift (optimum fineness ratio)	C_z	= 0.5
& cruise Mach number (high speed)	M_o	= 0.82
coefficient of lift	C_z	= 0.4

Thanks to transonic technology, the relative wing thickness should reach 15% at the root and 12 to 13% on the outside. This is a considerable increase compared to the A300 which has a constant relative thickness of 10.5% over the entire span and a sweepback of more than 3° at the trailing edge.

Owing to the large aspect ratio of the wing, its design was first based on a careful drawing of a basic profile presenting the required aerodynamic characteristics.

2.2 - Basic Profile

The conditions of adaptation of such a profile are based on the simple laws of a sweptback wing with an infinite span:

3

$$M_{o_{2D}} = M_{o_{3D}} \cdot \cos \varphi_{25\%}$$

$$c_{\ell_{2D}} = \frac{c_{\ell_{3D}}}{\cos^2 \varphi_{25\%}}$$

Factor 1.2 includes all three-dimensional effects of span limits for an aspect ratio of 10. With mean values extracted from the aerodynamic wing conditions indicated in the preceding chapter, the following conditions are derived:

Mach number $\quad M_{o_{2D}} = 0.73$

coefficient of lift $\quad c_{\ell_{2D}} = 0.65$

$\varphi_{25\%}$ being equal to 25°.

An iterative procedure has been adopted for the design of this profile for which we have looked for a "plateau" type upper surface pressure distribution followed by an isentropic recompression, while the high coefficient of lift is obtained by a high rear loading. /4 This leads us to the definition of the DFVLR-R4 profile |9| with a relative thickness of 13.5% and the geometric characteristics of which are shown in figure 2. Shown also, for illustration, (fig.3) are the pressure distributions obtained in the vicinity of an adaptation point by calculation |10| and in the TWB wind tunnel of the DFVLR.

2.3 - Geometric Characteristics of the Wing

Based on this profile which must assure the desired type of recompression, the wing design is formed with the following objectives:

-to obtain a minimum induced drag by an elliptical lift distribution along the span;
-to obtain along the wing surface a network of isobars parallel to the lines at X/C = constant.

To accomplish this, the wing twist law has been determined using a reverse method of vortex network [11] with an elliptical lift distribution by starting with a load distribution corresponding to that of profile R4 at the adaptation point. The external part of the wing (beyond the trailing edge break) is obtained by projecting the basic profile in the wind bed (by the cosine of sweep angle φ $25°$ χ) and by its adjustment to the calculated twist angle $\mathcal{E}_v$. For the definition of the profile at the root, iterative calculations have been performed around the entire configuration using a transonic method of small disturbances [12] by applying the above-mentioned concept of straight isobar lines.

Finally, the DFVLR-F4 wing is defined geometrically from 4 definition sections presenting the following characteristics:

	$\eta = 2y/b$	c/c	$\mathcal{E}_v$
1 - root	0,126	0,15	4,5°
2 - trailing edge break	0,4	0,122	1,8°
3 -	0,7	0,122	0,9°
4 - tip	1,0	0,122	-0,5°

The relative thickness laws and the wing twist are shown in figure 4. In order to obtain a simple geometry, a linear interpolation procedure has been adopted between the 4 design sections.

This wing is integrated with the fuselage in low position with a dihedral angle of 4.8°.

3 - EXPERIMENTAL STUDY IN THE S2MA WIND TUNNEL

This study was preceded first by a 1/38 scale half-model ($\approx$ 0,5877 m) in the Göttingen wind tunnel of DFLR (see ref. then by the first experimentation of the complete model (same scale) at NLR in the HST wind tunnel. It should be noted that the construction of the full model and the execution of this test correspond to GARTEUR operations.

As with the case of the HST wind tunnel, the full model was mounted at S2MA on a Z-shaped sting using a 6 component balance. The right wing is equipped with 252 pressure inlets distributed into 7 measuring sections, plus 44 pressure inlets placed along a vertical plane to the fuselage. Moreover, the left wing received an instrumentation for unsteady measurements (1 root gage, 2 accelerometers, 7 "Kulite" pressure transducers) and 14 colored fluid transmitters for buffeting investigations.

The tests were performed at the maximum perforation rate <u>/5</u> of the test section (6%). Under these conditions, the wall effects are known to be very small. Considering its dimensions, at the cruising point of model F4, we can expect to have corrections of about:

$$\Delta M = \pm 0.003 \quad \text{in Mach number}$$

$$\Delta \alpha = \pm 0.03° \quad \text{in incidence}$$

Nevertheless, in order to meet the abovementioned quality conditions, corrections are made of wall effects, of the pressure gradient in an empty test section and of the sting effect.

In order to assure an interference of shock wave - turbulent boundary layer, which is considered to be indispensable, it is necessary to start the transition on the upper surface and on the undersurface of the wing using the nominal Reynolds number of these tests ($R_c = 3.10^6$, and the aerodynamic reference chord c = 0.1412m). The next chapter describes a few problems connected with this transition initiation.

3.1 - Evaluation of the Effects Caused by the Initiation of the Transition on the Wing

The transition initiator retained for all tests of model F4 is a carborundum band 3 mm wide which has the same position on the upper skin and on the lower skin for all tests. On the top skin, it is selected as a function of the shock wave positions at the adaptation point and the surrounding area. It is the result of a

6

compromise between a position too far forward and a position too far backward which would prevent the formation of a homogeneous turbulent boudnary layer upstream from the shock. On the undersurface, this position is determined as a function of the pressure gradient in order to avoid too much reduction in the rear loading caused by a thickening of the boundary layer. The selection made for the F4 wing is illustrated in figure 5.

We now have to determine the optimum size of carborundum for initiating the transition on the band without excessive thickening of the turbulent boundary layer in order to avoid a parasitic drag. This operation is performed in an industrial wind tunnel using visualisations of the transition by a sublimation technique. This investigation is usually conducted with the cruise Mach number for a coefficient of lift Cz in the vicinity of the appearance of bufetting. A critical analysis of the selection performed at S2MA has been tried at DERAT by a purely two-dimensional approach using an empirical criterion of optimum initiation [13]. The result is shown in figure 6 for a measuring section situated at $x/b = 0.636$ at the upper surface and at the undersurface in the case of cruise conditions. The roughness heights seem to be close to their optimum values. The excess thickening of the boundary layers is therefore evaluated to be very small.

Nevertheless, considering the rather low Reynolds numbers that can now be obtained on transport aircraft models, more effort is needed to develop a more reliable technique of transition onset in a wind tunnel and to improve the prediction means in this regard of the device used on the created turbulent boundary layer.

The general consequences of transition initiation may be brought to light by a comparison with tests of natural transitions. For illustration, figure 7 shows the pressure fields on the wing in natural transition ($\sim$) and the initiated transition ($\circ$) for Mo = 0.75 and $c_z = 0.5$, which corresponds to one of the 3 cases of calculation selected by the GARTEUR research team which we will return to in chapter 4. Notwithstanding the noticeable

7

reduction of the rear loading at the external wing undersurface in <u>/6</u> TD, the shock wave position at the upper surface seems to be hardly affected by the initiation. On the other hand, the variation of the coefficient of pressure at the trailing edge of the section situated at $2X/\ell = 0.409$ at this Mach number and also at the cruise Mach number (fig.) diverges at C_z that are much lower in TC than in TN. Since this divergence is expressed by the appearance of a separation at the trailing edge, the Cz appearing with buffeting is also lower in TD than in TN. Likewise, we can see in figure 9 that the fineness ratio, at the cruise Mach number, undergoes a loss of about 10% at the cruise Cz relative to the configuration in TN.

3.2.- Aerodynamic Performances

To have a general idea of the aerodynamic quality of the configuration under study (in TD), the drag divergence limit should first be studied in a plane Cz, Mo. This requires the study of the drag coefficient variation Cx as a function of the Mach number at Cz (figure 10). In passing, it may be observed on this figure the absence of a noticeable precritical drag. The determination of the drag divergence from these curves has been performed using the usual criterion

$$\partial c_x / \partial M_o = 0.1$$

The result obtained is shown in figure 11 and shows in particular that the target cruise point for the flight at an optimum fineness ratio is situated below this limit that physically expresses the presence of a supercritical flow with the appearance of shock waves.

Finally, in order to evaluate the induced drag, it is convenient to examine the experimental curve

$$C_x = f(C_z^2)$$

8

The slope of this curve relative to the optimum theoretical value

$$\frac{\partial c_x}{\partial c_z^2} = \frac{1}{\pi \Lambda}$$

is a quality index. Figure 12 presents the result obtained at the cruise Mach number, the slope ratio being $\mathcal{k} = 0.882$.

The aerodynamic quality of a project may also be expressed in the Bréguet formula relative to the distance that the term can cover

$$c_z / c_x \cdot M_o$$

the maximum of which is researched for the cruise point. A plotting of lines at the same level, extracted from the set of stress measurements, in plane Cz, Mo (figure 13) illustrates that this condition is quite satisfactory in the present case.

One last point concerning the limit of a buffeting appearance is as follows: considering the model equipment used, several types of measurements allow us to make an evaluation of this limit:

-steady measurement using the balance: $c_z = f(\alpha)$; the appearance of buffeting is determined at $\Delta\alpha = 0.1°$ beyond the linear variation of this curve,

-unsteady measurements (RMS values within a given frequency /7 band) by the balance (dynamic roll $c_{\ell\, RMS} = f(\alpha)$, a bending gage at the root and an accelerometer integrated in the wing. In these cases, which correspond to various structural responses, the appearance of bueffeting is diagnosed by the signal divergence, i.e. a sudden increase in its intensity when the incidence increases beyond a certain value.

Figure 14 shows that the range formed by all limits thus found is very wide and its interpretation is not easy. Nevertheless, the limit deduced from the curves of lift are likely to be pessimistic in a case such as this one for which the important viscous effects affect the flow on the airfoil.

If a first problem in the study of buffeting is an accurate
determination of the appearance of this phenomenon, an even great-
er problem is quantification. An attempt is being made to implement
the very simple, but also very controversial Mabey method [14].

4 - PREDICTIONS BY CALCULATION AND COMPARISON WITH EXPERIMENTS

The conditions for the calculations to be performed on the
configuration under study were suspended after the experiments on
the model at NLR were completed. The selection made on cases in
the vicinity of the cruise point exempt from pronounced local separations:

	1	2	3
Mach number Mo	0.75	0.75	0.77
coefficient of lift Cz	0.5	0.6	0.5
or incidence α	0.10	0.84	-0.01

In order to account for deformations subjected by the airfoil
under aerodynamic loading, a minor correction of the twist law
(chapter 2.3) has been made as a result of a theoretical evaluation
at the NLR.

4.1 - Supercritical Flow on the Wing

Calculations have been performed at ONERA, as is the case with
most participants, by processing the airfoil separately as an "exposed"
airfoil. These are perfect fluid calculations using a relaxation
method to solve the equation of full potential in a non-conservative
form. This method isddescribed in detail in [15]. The code of
calculation has, nevertheless, been constantly improved and it now
exists in a more operational form.

Since a calculation - Cz experiment comparison is likely to under-
go considerable effects of compensation, the calculations have been
performed at a given incidence. This method of procedure does not
favor a comparison with the experiment, but it does make it possible
to evaluate important viscous effects that are expected in view of

the high rear loading of the wing.

Calculations are performed using a boxed meshing technique, the finest mesh of which is 130 x 32 x 30, or 124,800 points, while the flow on the wing is described by 20 sections along the span with 84 points in each (42 at the upper and lowersurface). The meshing, of parabolic type, develops spanwise. Figure 15 shows details of the sections closest to the root and tip of the F4 wing. It may be seen that the sheet outlining the slip-stream straightens as we move downstream from the wing.

The variation of the maximum residue along the iterations and the convergence of the lift are shown in figures 16 and 17 for the case of the first calculation. The last figure indicates that the result obtained has not completely converged, in spite of a 185 mn computer time on the Cyber 170-750 computer.

The solution obtained is shown by iso-Mach lines at the upper surface (fig.18), then by the pressure field viewed in perspective along the upper surface and on the undersurface (fig.19). On the upper surface, we may see the presence of a widely extended super-critical zone with a high plateau preceded and followed by relatively important recompressions and, on the undersurface we may see the high rear loading, particularly on the external part of the wing.

The comparison of these pressure distributions with the experiment on figure 20, however, is not satisfactory. It is not satis-factory in the fine description, with in particular the absence of a definite shock wave and a too high rear loading in the calcula-tion, or at the level of the coefficients of local lift $c_{z\ell}$, the theoretical values of which are clearly too high. The span load distribution (fig.21) confirms the high overestimation of the calculations, although the appearance of the curves are quite sim-ilar. Furthermore, the lack of agreement in the calculation-exper-iment comparison appears also in the other two cases treated.

It should be remembered that the transonic calculations per-formed do not include the presence of the fuselage and the viscous

effects. In the next chapter we will try to evaluate the respective role of each of the two factors.

4.2 - Evaluation of the Influence of the Fuselage and Viscous Effects

In order to determine the respective influences of the fuselage and of the viscous effects on the airfoil, the case of a subcritical flow was prepared. The following conditions were selected:

Mach number $\qquad$ Mo = 0.60

incidence $\qquad$ $\alpha = 0.7°$

In order to evaluate the influence of the fuselage, we used a method of singularities developed by Aérospatiale [16] in which the effect of thickness is determined by a surface distribution of sources, whereas the lift effect is obtained using a doublets distribution on the outline of the airfoil.

The calculations performed are, of course, concerned with the wing-fuselage combination, the quantification of which is shown in figure 22, then with the fuselage separately and the wing separately. Two calculations were performed for the latter:

-one for the wing extrapolated to the symmetry plane,
-the other for the exposed wing as adopted for transonic calculations.

First, the wing to fuselage interferences are shown by comparing the pressure distributions (fig.23) obtained in the symmetry plane for complete system configurations and for the fuselage separately. An excellent agreement between calculations and experiment may be noted.

The fuselage to wing interferences are shown in figure 24, where a comparison is given, first, of the span loading distributions calculated on the entire configuration and on the extrapolated wing. It may be observed that the theoretical lift of the extrapolated

wing overshoots that of the full configuration by some 8%.
The calculation-experiment comparison of the local lift distri-
bution on the full system brings to mind that of the supercritical
case (fig. 21). The calculated lift exceeds the experimental value
by 30%.

Another concern is to bring to light the benefits of exposed
wing calculations compared to full configuration calculations. The
answer may be found in the results presented in figures 25 and 26.
By comparing the lift distributions obtained by the method of singu-
larities, we may detect, at the wing level, relatively few differences
between the full configuration and the exposed wing which are ex-
pressed by a lift deficiency in the case of the exposed wing of
about 3.5%. Moreover, the result of a calculation of the exposed
wing using the transonic method agrees perfectly with the result
given by the method of singularities. The pressure distributions
calculated on the full system and on the exposed wing by using both
methods confirms the idea that the concept of the exposed wing in
the calculations is acceptable, at least in the subcritical case.
Furthermore, a few published results [17], [18] tend to show that
this observation is also true for supercritical flows.

To bring to light the influence of viscous effects on this con-
figuration, a two-dimensional approach has been tried by using
a section at mid-span from the wing. The calculation code used
solves the entire equation of potential in connection with the
evaluation of the boundary layer using an integral method [19]
In an iterative calculation process, the geometry is corrected of
displacement effects, with the convergence intervening a few steps
later.

For the example treated here (fig. 27), the two-dimensional
calculation was performed by beginning with the perfect fluid of
the coefficient of local lift determined by three-dimensional cal-
culation. The agreement of the pressure distributions thus calcu-
lated with the experiment is good, except at the undersurface at
the rear loading level. Compared to the experiment, the calculation

of the perfect fluid leads to an overestimation of the local lift by 26%, that of the viscous fluid leads to on overestimation of only 4%. This proves that the influence of viscous effects on the F4 system is considerable and explains the poor quality of direct comparisons of perfect fluid calculations and experimentation.

5 - CONCLUSION

The DFVLR-F4 model, designed within the framework of the German ZKP research operation, has been selected by a research team of GARTEUR as a support for transonic studies of a wing-fuselage system used to represent a civilian transport aircraft. Experimental results are expected to be obtained in four of the larges transonic wind tunnels of Europe to be used as a basis of evaluation of operational transonic calculation methods or of those being developed.

We may at this time conclude from results already collected in the S2MA wind tunnel that the aerodyanmic conditions of the project are satisfactory. However, the initiation of the boundary layer transition on the wing, which is imperative for obtaining turbulent boundary layer - shock wave interferences on the top skin using Reynolds number $c_r = 3.10^6$ results in a few losses from the point of view of performances.

Furthermore, the calculation - experiment comparisons performed at ONERA stress the presence of important viscous effects on this configuration. On the other hand, the influence of the fuselage does not seem to be a major obstacle for a comparison of experimental results with calculation results obtained on only the wing.

14

[1] G.HECKMANN -
     **Use of the finite elements method to study wing-fuselage
     interferences of a FALCON type aircraft at Mach = 0.79.**
     AGARD CP 285 - Paper n° 3, 1980.

[2] W.SCHMIDT -
     Aerodynamic subsonic/transonic aircraft design studies by numerical
     methods.
     AGARD CP 285 - Paper n° 9, 1980.

[3] R.DILLNER, C.A.KOPER, Jr -
     The role of computational aerodynamics in airplane configuration
     development.
     AGARD CP 280 - Paper n° 15, 1980.

[4] P.T. LYNCH -
     Recent applications of advanced computational methods in the
     aerodynamic design of transport aircraft configurations.
     ICAS - Proceedings, Vol. 1, Paper B 2-02, 1978.

[5] D.A.CAUGHEY, A.JAMESON -
     Recent progress in finite volume calculations for wing fuselage
     combinations.
     AIAA Paper 79-1513, 1979.

[6] G.REDEKER, N.SCHMIDT -
     Design and experimental investigations of a wing for a transonic
     transport aircraft .
     DGLR - Paper 78-085, 1978.

[7] G.KRENZ, B.EWALD -
     Transonic wing technolgy for transport aircraft.
     AGARD CP 285 - Paper n° 12, 1980.

[8] G.REDEKER, N.SCHMIDT, R.MULLER -
     Design and experimental verification of a transonic wing for a
     transport aircraft.
     AGARD CP 285 - Paper n° 13, 1980.

[9] G.REDEKER, R.MULLER -
     Design and experimental verification of two supercritical airfoils .
     DGLR - Paper 78-025, 1978.

[10] F.BAUER, P.GARABEDIAN, D.KORN, A.JAMESON -
     Supercritical wing sections II.
     Springer Verlag, New-York, 1975

[11] H.KORNER -
     Ein Verfahren zur Berechnung der Verwindung und Verwölbung des Flügels
     bei vorgegebener Lastverteilung unter Berücksichtigung des Rumpfes.
     WGLR ....., ...

[ ] [ ] ...., F.HISMAN -
Mixed configurations in relaxation methods for three-dimensional
transonic potential flow.
.... - Paper n° 76-22, 1976.

[ ] [ ] D.ARNAL, J.C JUILLEN, M.OLIVE -
Synthesis of transition initiation results using
rough bands of carborundum. Unpublished Document.

[ ] [ ] . .C.MABEY -
An hypothesis for the prediction of flight penetration of wing buffeting
from dynamic tests on wind tunnel models.
ARC.CP 1171, 1971.

[ ] [ ] J.J CHATTOT,C.COULOMBEIX, C.da SILVA TOMÉ -
Transonic flow calculations around wings.,
Aérospatiale Research No. 1978-4, 143-158, (1978).

[ ] [ ] M.YIRTLI -
Calculation of subcritical potential flows around
three-dimensional bodies using a method of singularities.
Unpublished document.

[ ] [ ] R.L.JHINSON, K.P.BURDGES -
An evaluation of three dimensional transonic
codes using new correlation tailored test data.
AIAA - Paper 80-0003, 1980.

[ ] [ ] K.J.YU -
Grid generation and transonic flow calculations
for three-dimensional configurations.
AIAA-Paper 80-1391, 1980.

[ ] [ ] J.BOUSQUET -
Two-dimensional transonic calculations with
boundary layer. 11th AAF Symposium, 1974.
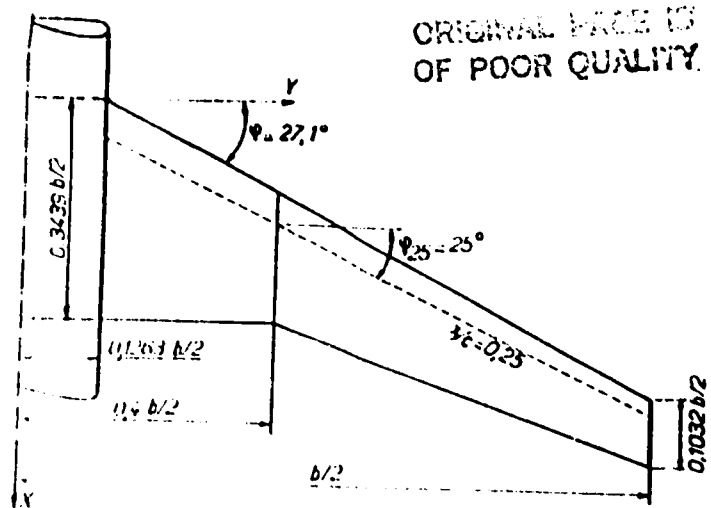
Fig. 1 - Planar Shape of the DFLR-F4 Wing.

Geometric parameters:

aspect ratio	Λ	=9.5
taper ratio	λ	=0.3
leading edge sweep	φ	=27.1°
fuselage radius	$2y_i/b$	=0.1263
trailing edge break	$2y_c/b$	=0.4
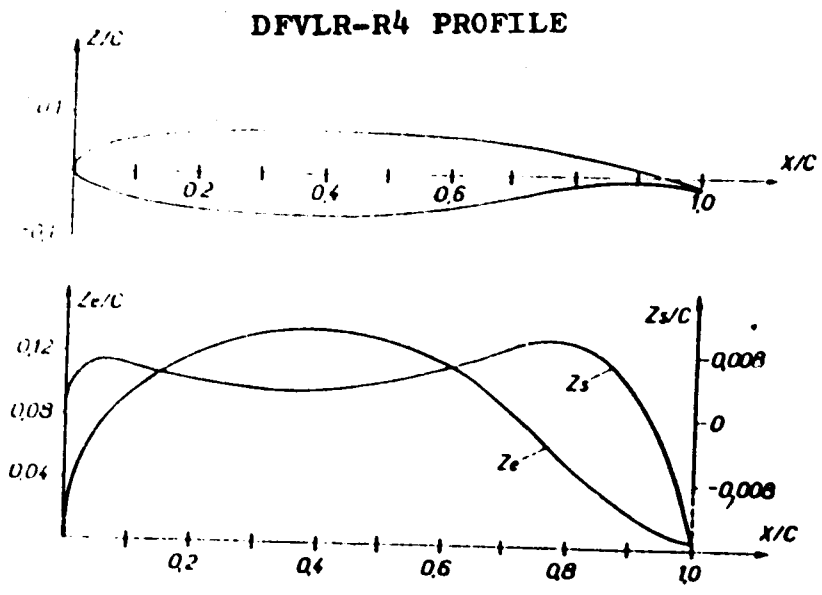
DFVLR-R4 PROFILE

Fig. 2 - Geometric Characteristics of the Basic Profile.

DFVLR-R4 PROFILE

$M_0 = 0,73$ $C_z = 0,6$
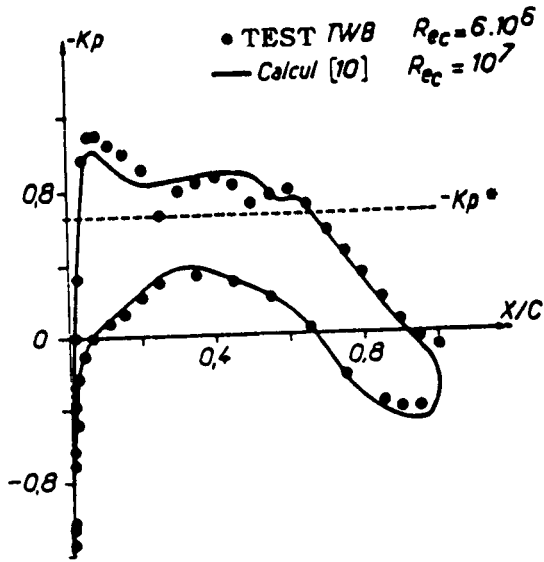
Fig.3-Theoretical & Experimental Pressure Distributions in the Vicinity of an Adaptation Point.

Design Sections:
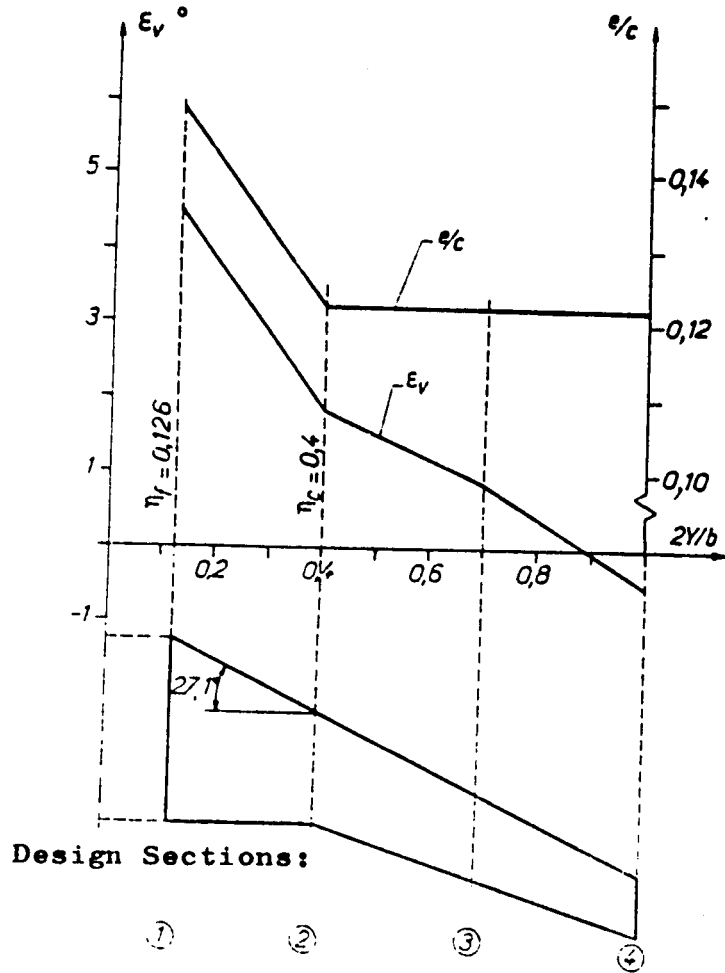
Fig.4-Relative Thickness Laws and Twist of the DFVLR-F4 Wing.

S2LA TESTS $Re_c = 3.10^6$

---- carborundum band
(width: 3mm)

$\eta = 0,409$

$X/C = 0,05$

$X/C = 0,15$

0,844

$X/C = 0,05$

Upper Surface
position: $x/_c = 0,05/0,15/0,05$
size: 220

Undersurface
position: $x/_c = 0,25$
size: 240

0,05

$X/C = 0,25$

0,409

$\eta = 0,844$
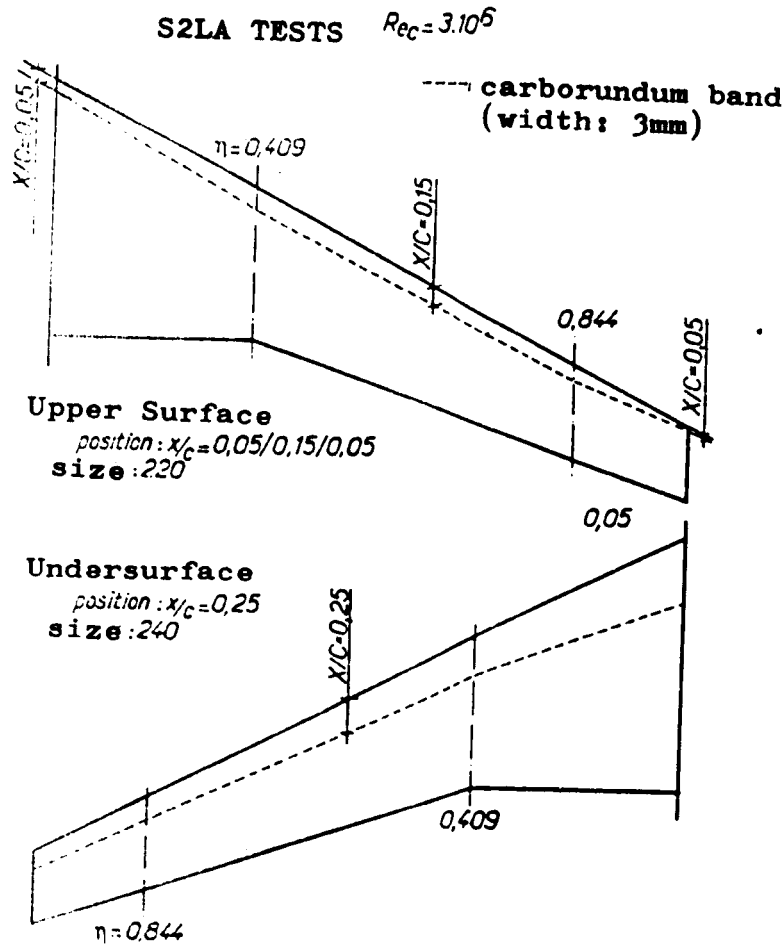
Fig. 5 - Wing Transition Initiator.

S2MA TEST $Re_c = 3.10^6$
$M_0 = 0,78$ $C_z = 0,5$

Re_R

Re_R

Section $2Y/b = 0,636$

undersurface □

upper surface ■

400

400

200

$dp/dx > 0$
$H_R = 2,75$

$dp/dx < 0$
$H_R = 2,47$

200

h/δ_{1R}

h/δ_{1R}

0   1   2   3

0   1   2   3
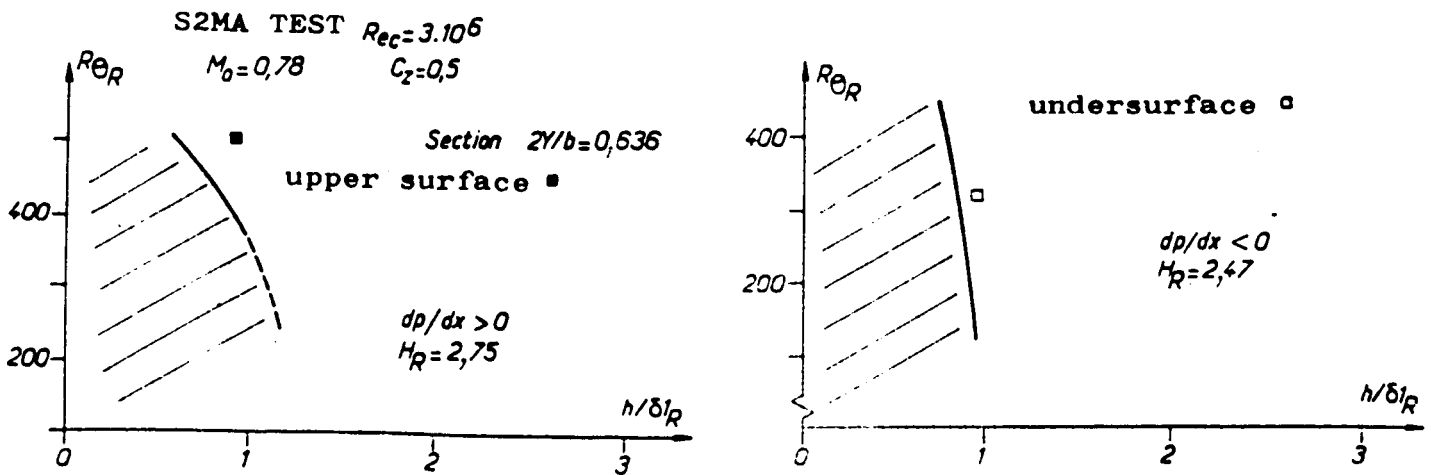
Fig. 6 - Application of the Transition Initiation Criterion to a
Rough Surface (DERAT [13]).

19
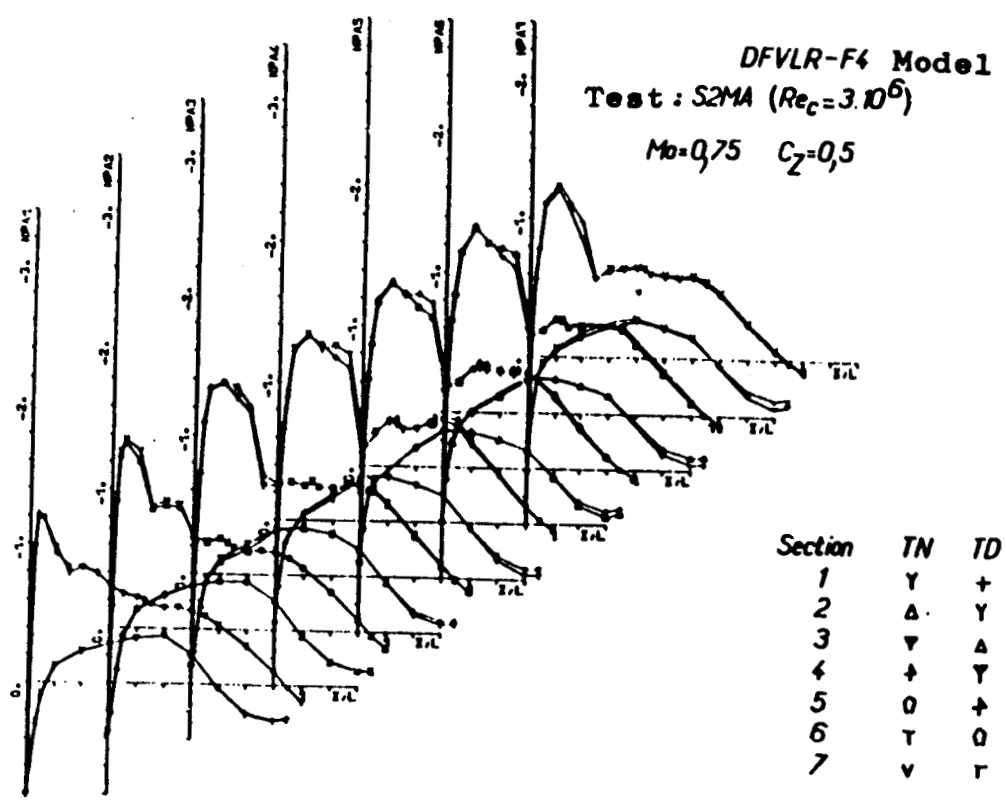
Fig.7-Example of Pressure Fields in Natural and in
Initiated Transition.
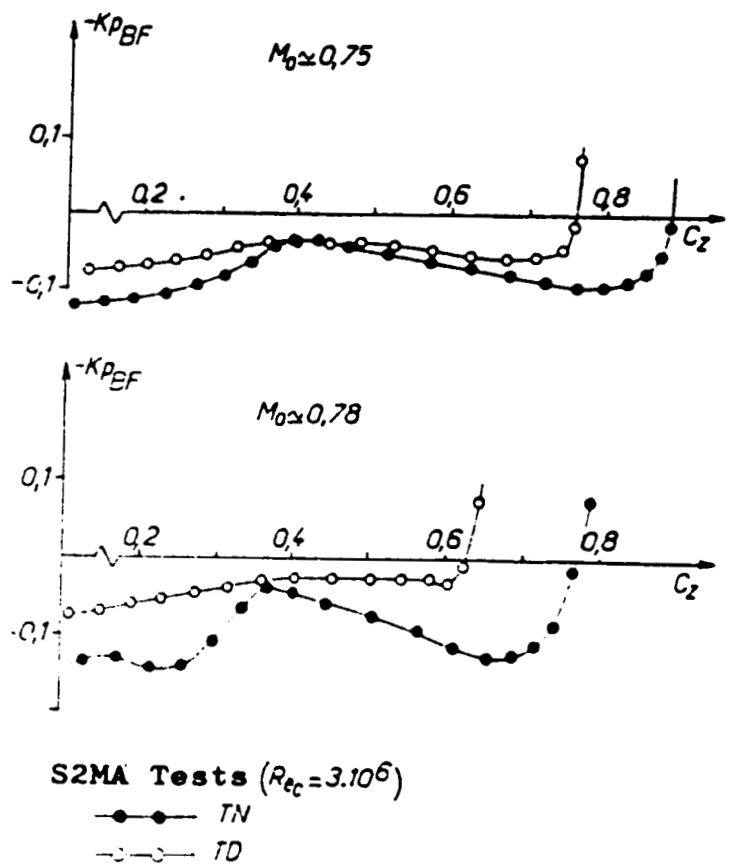
Fig.8-Effect of Transition Initiation on the Coefficient of
Pressure $K_{p\ BF}$ in section $2y/b = 0.409$.
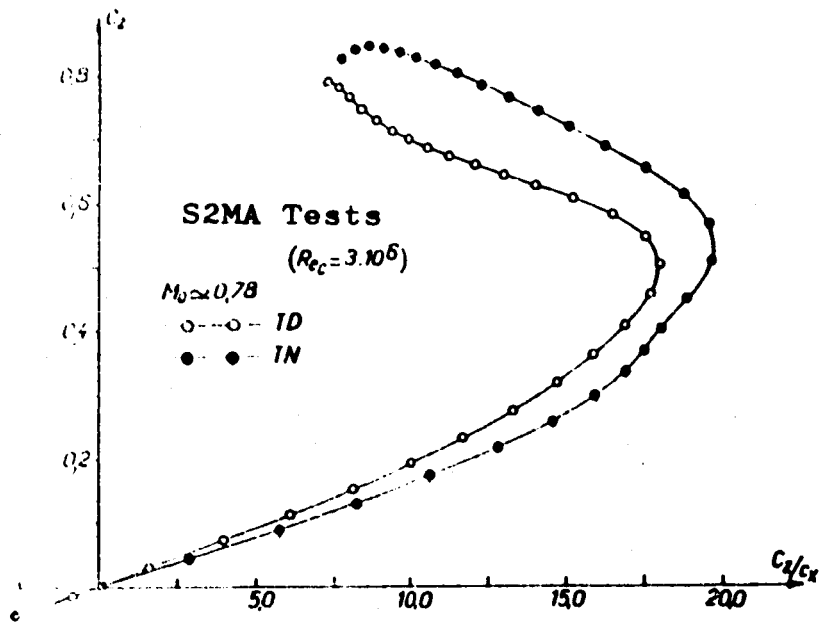
Fig.9- Finesse Ratios in Natural and Initiated
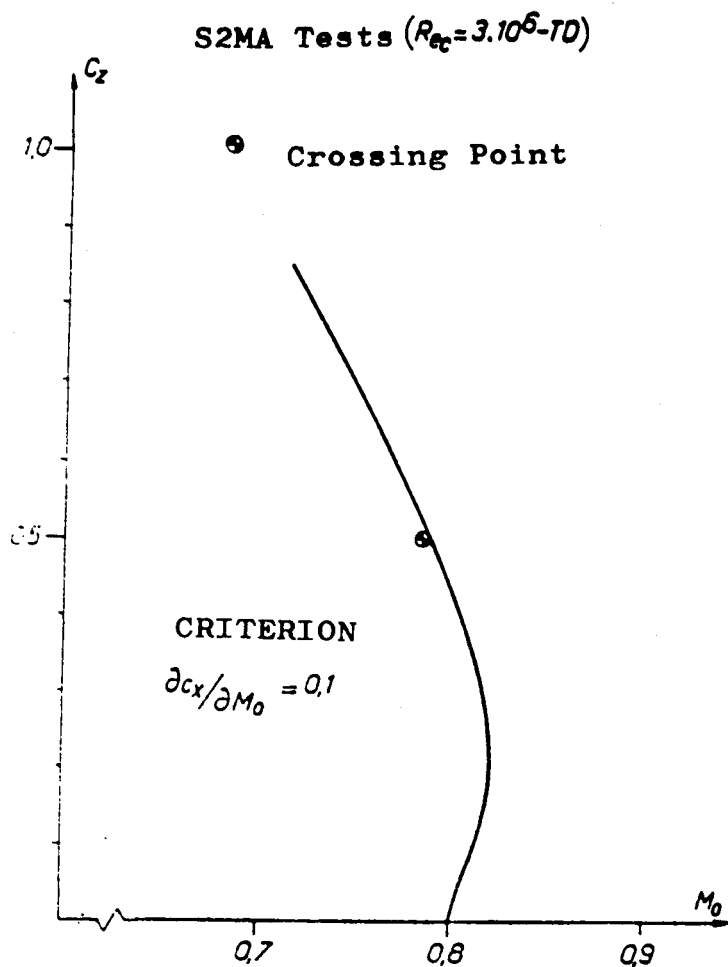Transitions.
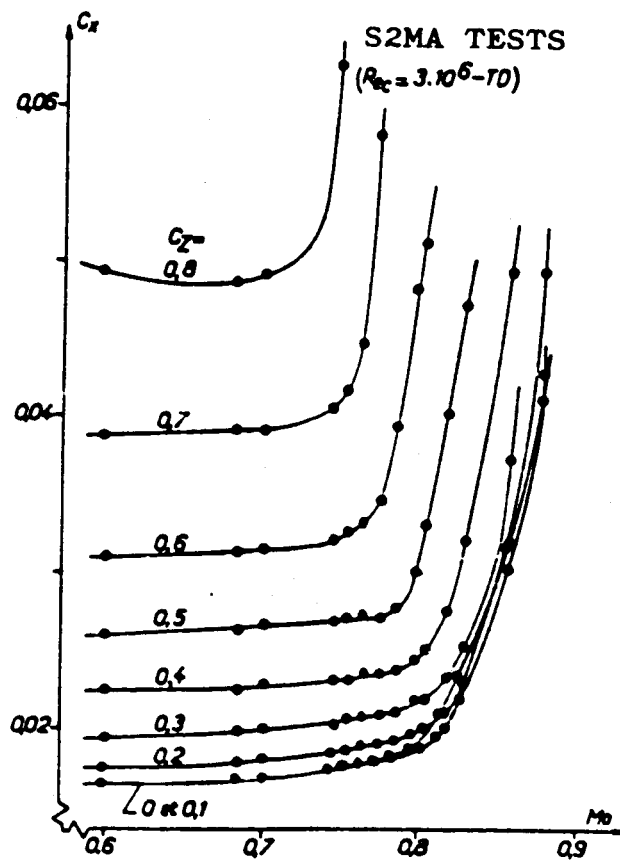
Fig.10-Drag Curves at C_Z=const.

S2MA Tests $(R_{e_c}=3.10^6-TD)$

C_z

⊕ Crossing Point

1,0

0,5

CRITERION

$\partial c_x/\partial M_0 = 0,1$

M_0

0,7 0,8 0,9

Fig.11-Drag Divergence Limit

S2MA TESTS $(R_{e_c}=3.10^6-TD)$

$M_0 \simeq 0,78$

C_x

0,04

0,02

$\partial C_x/\partial C_z^2$

━●━ 0,0380 $(k=0,882)$

------- 0,0335 $=\dfrac{1}{\pi\Lambda}$

C_z^2

0,2 0,4

Fig.12-Induced Drag.

DFVLR-F4 MODEL
2SMA Tests $(R_{e_c}=3.10^6-TD)$

C_z

●crossing point

Param $C_z/c_x \cdot M_0 =$ Constant

1,0

0,5

M_0

0,6 0,7 0,8
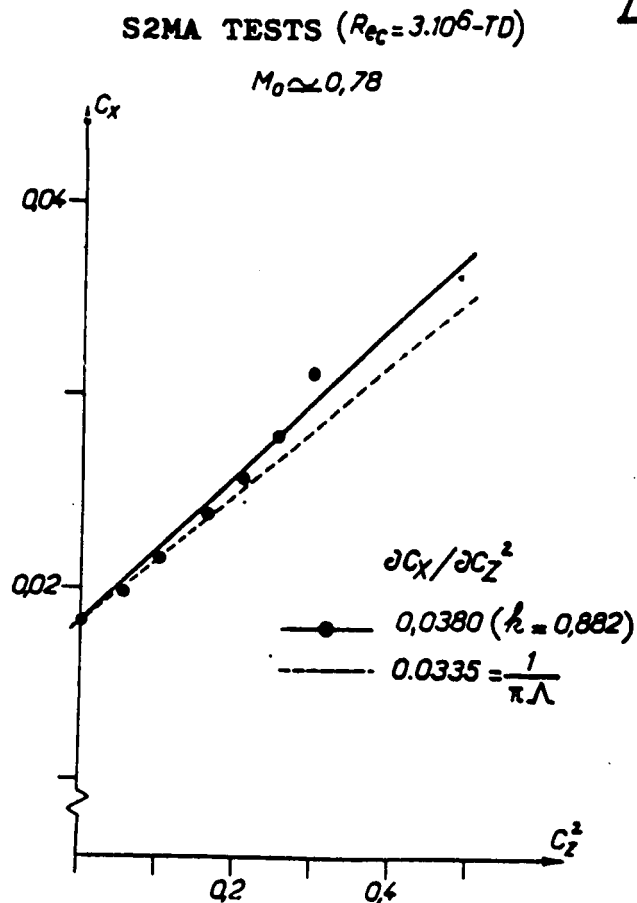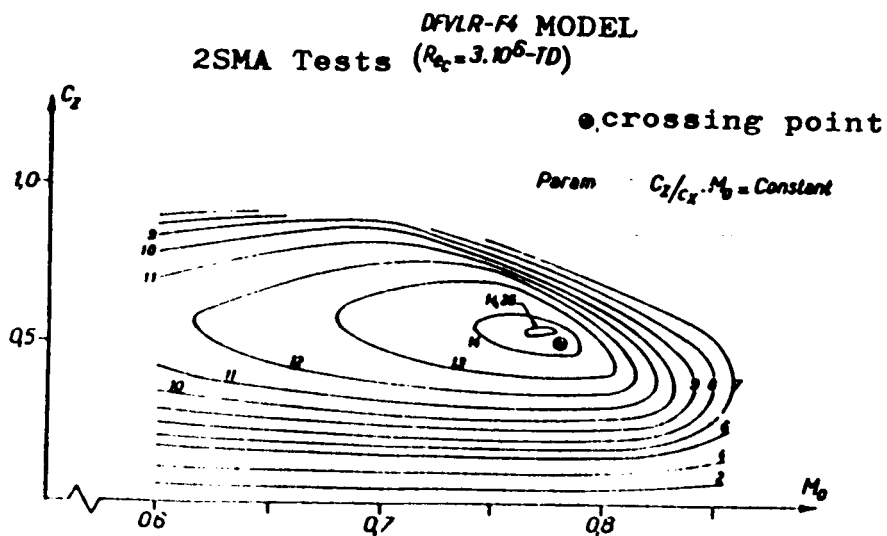
Fig.13-Aerodynamic Quality.

22

S2MA TESTS $(Re_C = 3.10^6 - TD)$
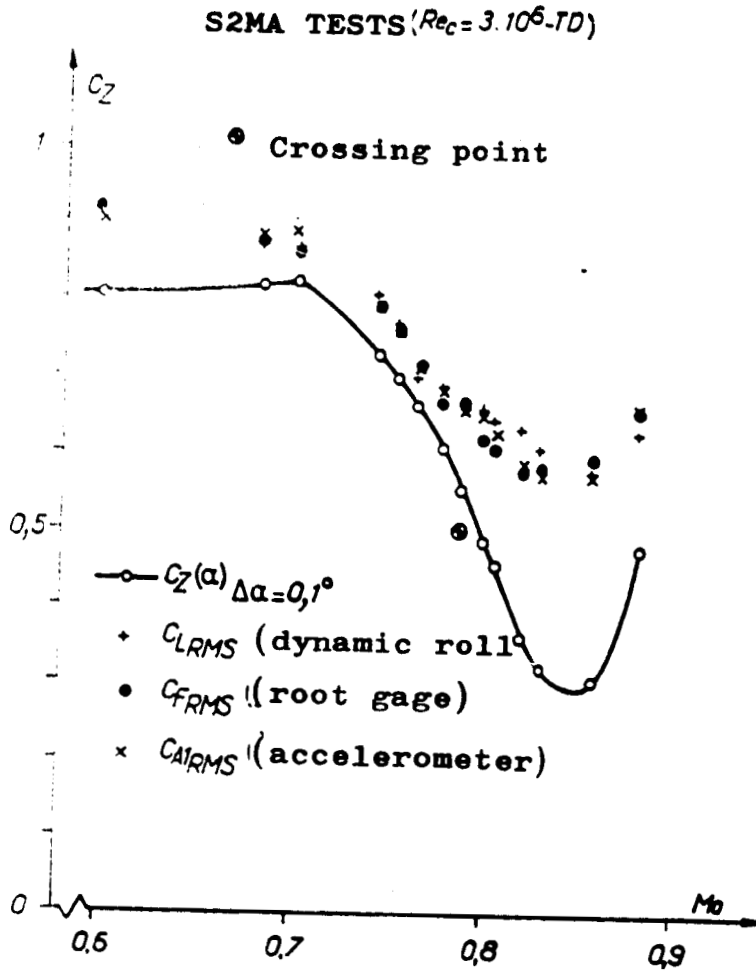
Fig. 14 - Limits for the Appearance of Buffeting.
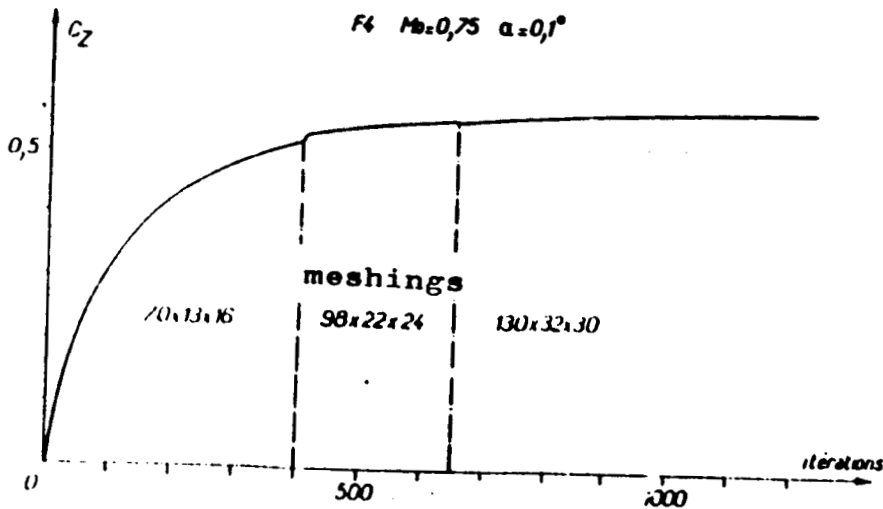
Fig. 17 - Lift Convergence

F4 Mo=0,75 α=0,1°

Ermax

meshings

70x13x16   98x22x24   130x32x30

10^{-3}

10^{-4}

10^{-5}

10^{-6}

——10'——|——25'——|———150'———|t.Cyber 170-75C

500   1000   1500 iter
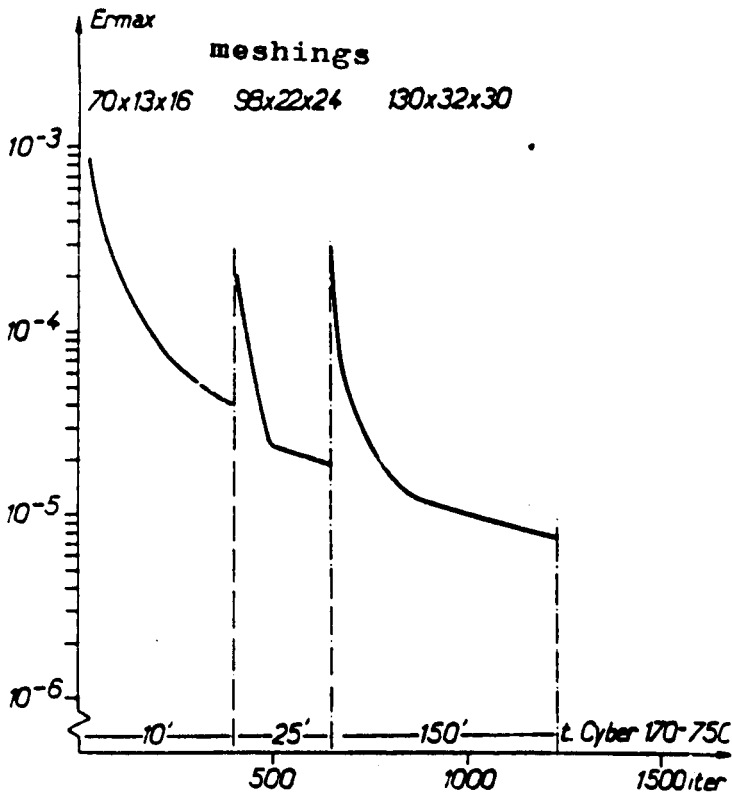
Fig.16-Maximum Error Variations.

F4
Mo=0,75
α =0,1°

Upper Surface

/18
/19

Fig.18-Iso-Mach Lines Calcu-
lated in the Vicinity
of a Crossing Point.

F4 Mo=0,75 α=0,1°

UPPER SURFACE

UNDERSURFACE

intrados

Fig.18-Field Pressure Calculated in the Vicinity of
the Crossing Point.

24

DFVLR-F4 MODEL $M_0=0.75$ $\alpha=0.1°$

		2Y/b	C_{z_i}	2Y/b	C_{z_i}
Calcul (FPE-NC)	——	0.323	0.726	0.847	0.741
Test (S2MA-$Re_c=3.10^6$)	•••••	0.331	0.585	0.844	0.535
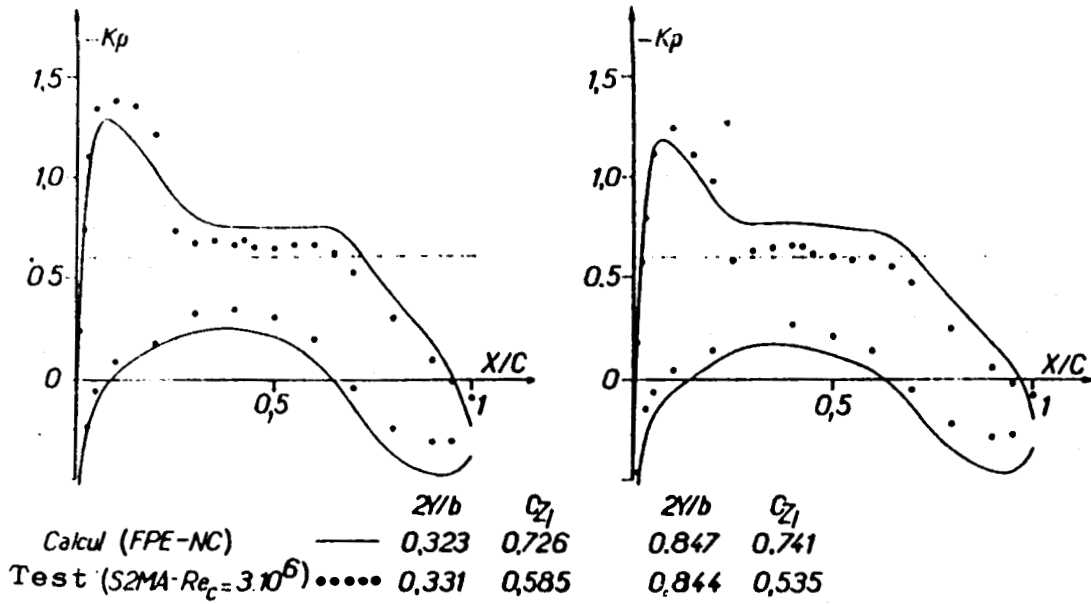
Fig.20-Pressure Distributions (Theoretical and Experimental).

DFVLR-F4 MODEL $M_0=0.75$ $\alpha=0.1°$

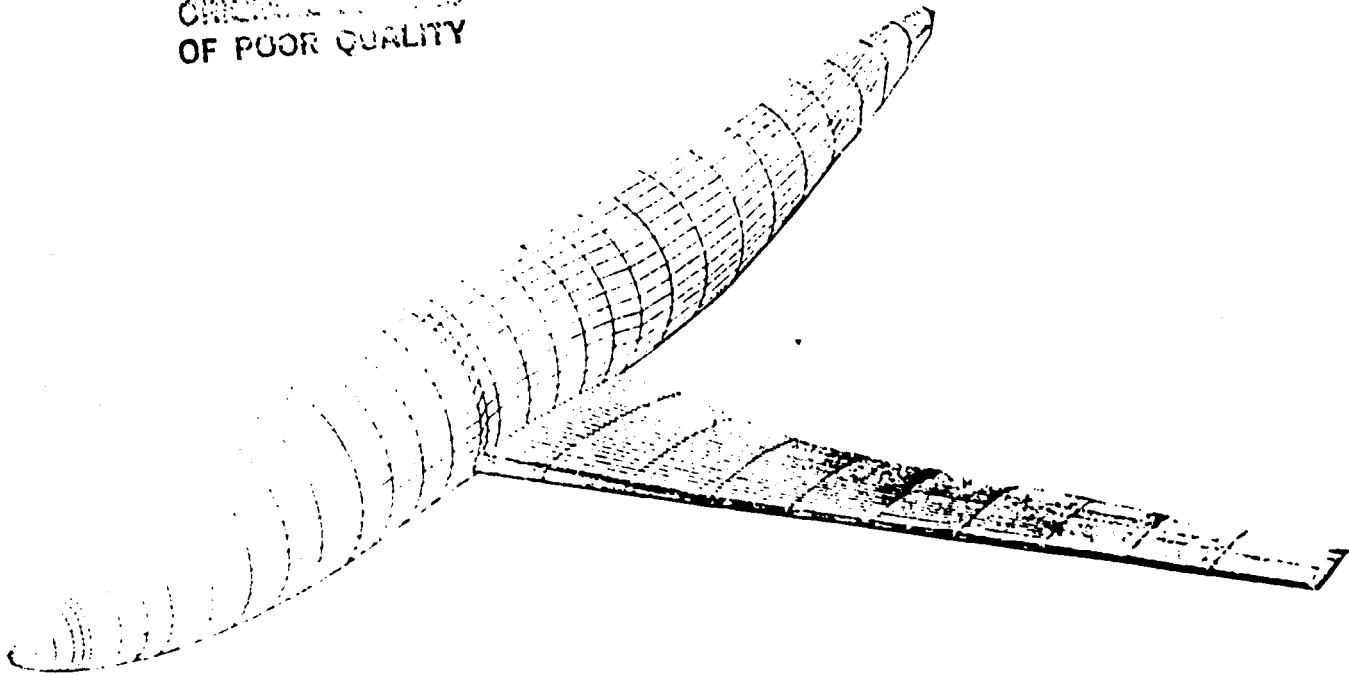|		C_z
Calcul (FPE-NC)	——	0.573
Test(S2MA-$Re_c=3.10^6$)	•••	0.50
(Wing part)		(0.42)
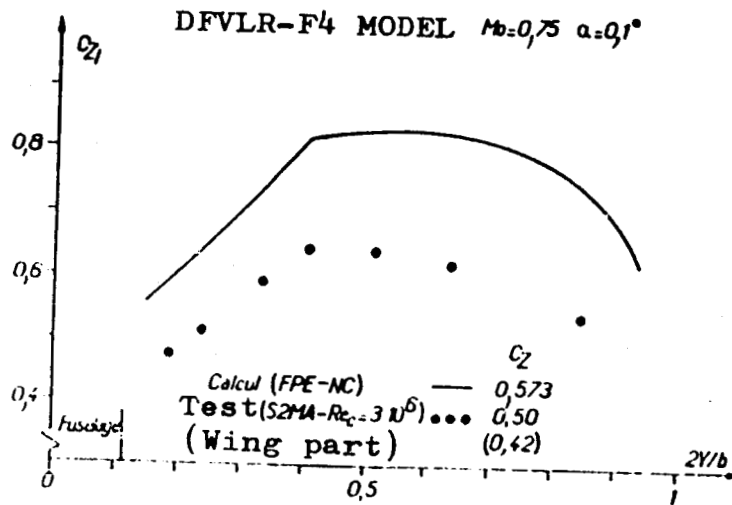
Fig.21-Span Lift Distributions.

Fig.22-Subcritical Calculations of the Wing-Fuselage F4 Model
Geometric Quantification.

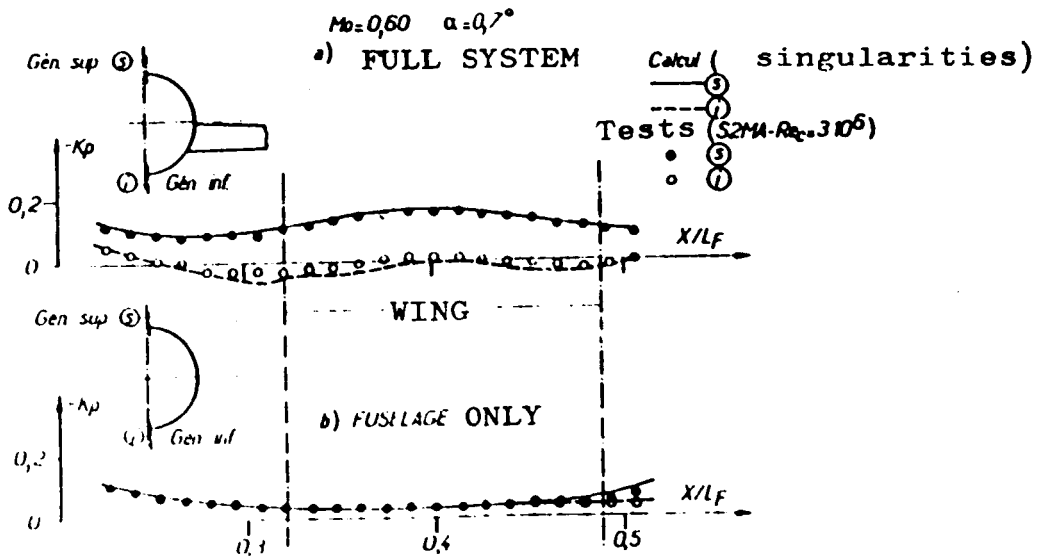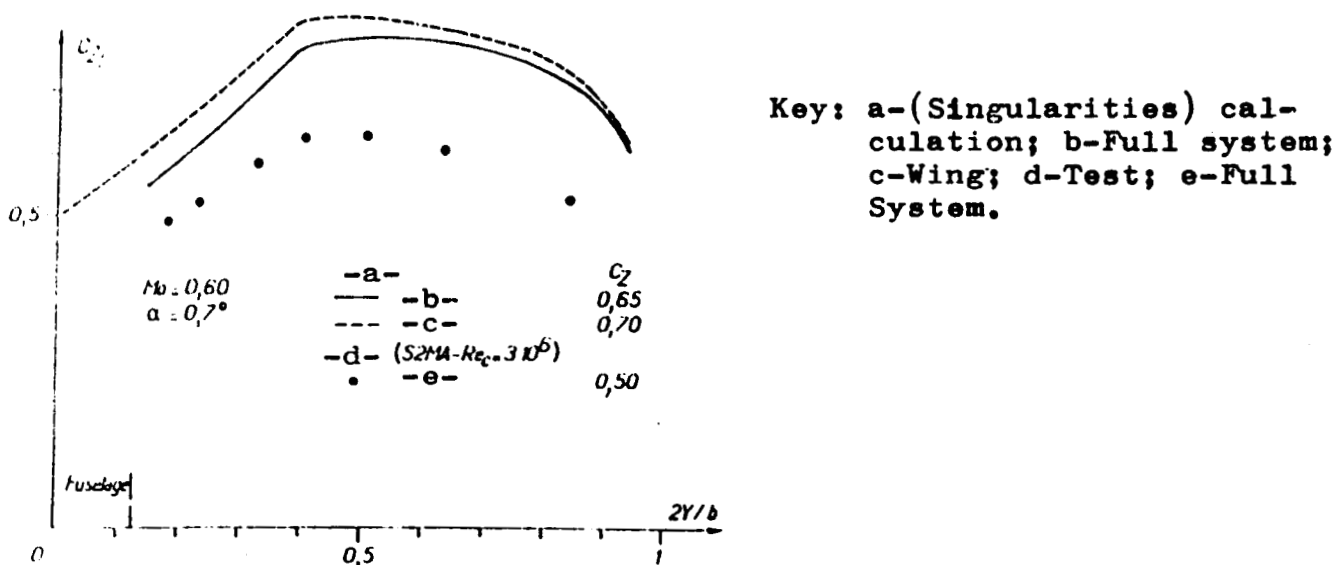Fig.23-Effects oi Wing-Fuselage Integration.

Key: a-(Singularities) cal-
culation; b-Full system;
c-Wing; d-Test; e-Full
System.

Fig.24-Effects of Fuselage-Wing Integration.

Key: a-Full system (singu-
larities); b-Wing part;
c-Exposed Wing;
d-Singularities.
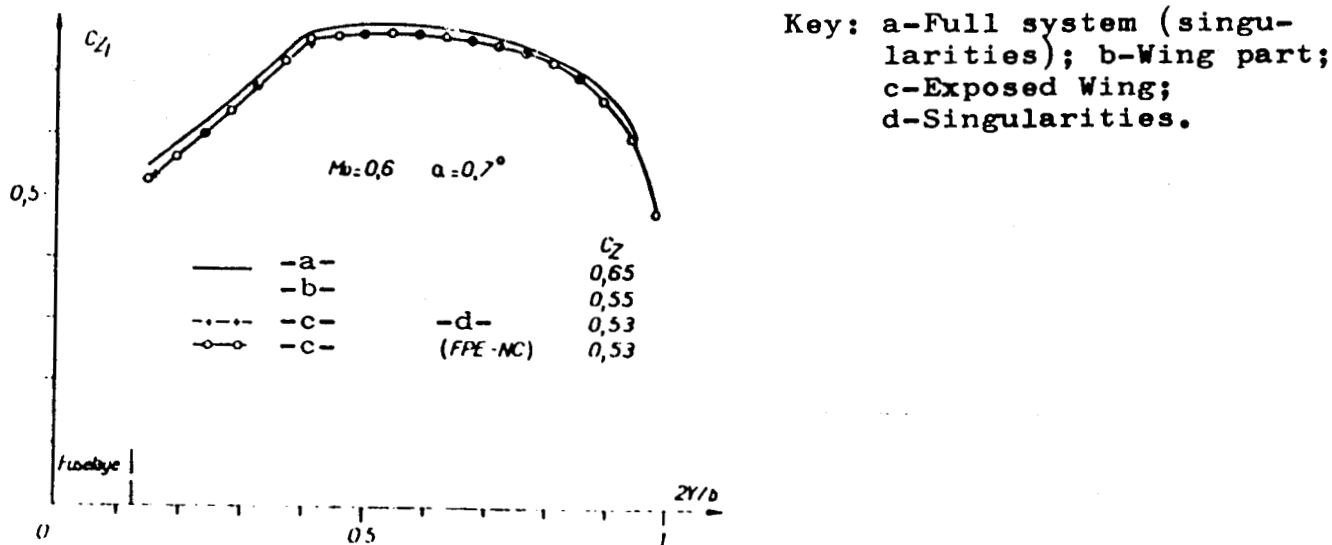
Fig.25-Influence of the "exposed wing"
design on the span lift distribution.

$M_0 = 0,60$ $\alpha = 0,7°$

Calculations
— Full system (singular)
-- Exposed wing (FPE)
Test (S2MA)
• Full system

$2Y/b = 0,24$

$2Y/b = 0,50$
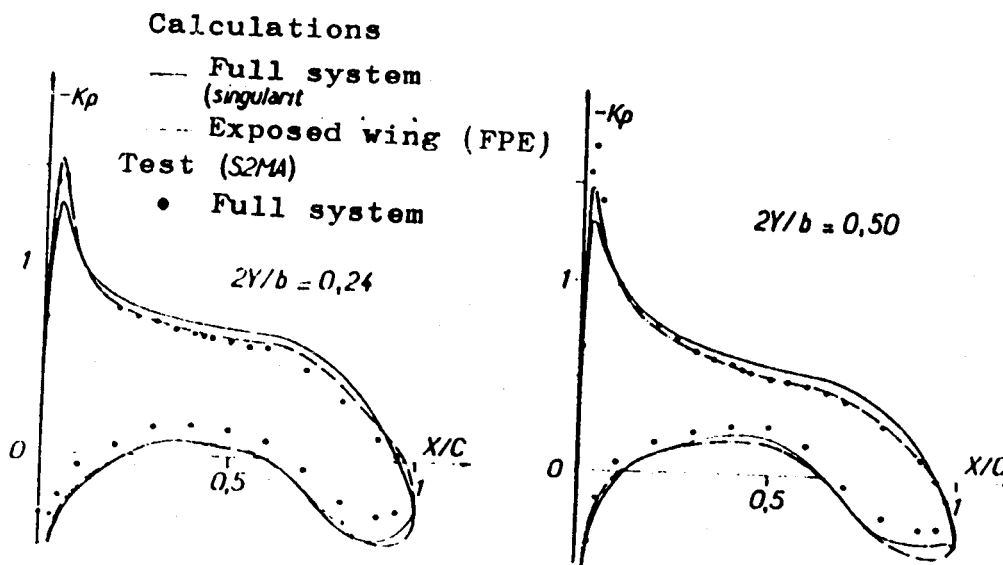
Fig.26-Influence of "exposed wing" concept on pressure distributions.

S2MA : $M_0 = 0,60$ $C_Z = 0,5$

	C_{Zl}
a)	
— -b-	0,786
-c-	
• -d-	0,622

	C_{Zl}
b)	
-- -e- (FPE)	0,786
--- -f- (FPE+CL)	0,646
• -g-	0,622
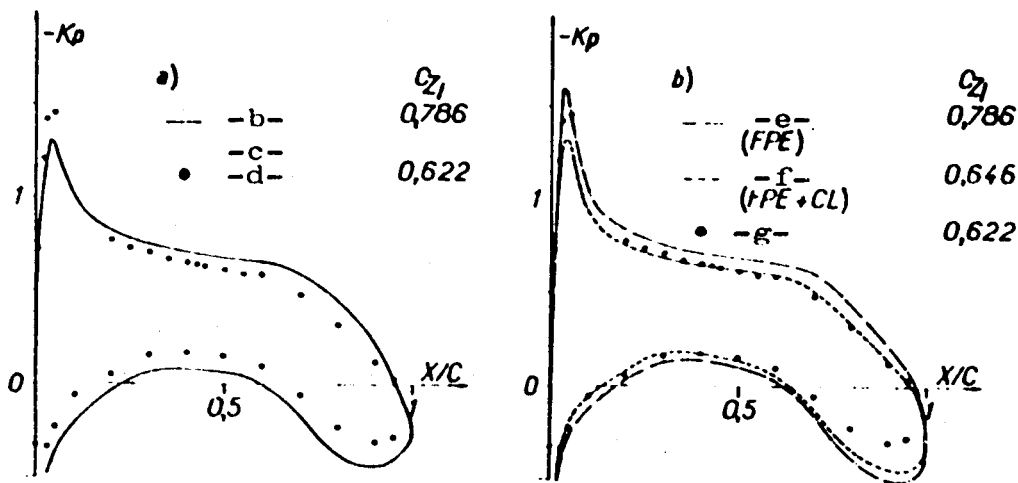
Key: a) 3D calculation; b) Perfect fluid c) (singularities);
d)Test *b) 2D calculations; e)Perfect fluid; f-Viscous
fluid; g Test.

28